Development of a novel dual-stage method for metaldehyde removal from water

Bing Tao and Ashleigh Fletcher*
Department of Chemical and Process Engineering, University of Strathclyde, James Weir Building, Glasgow, UK, G1 1XJ

Abstract

A dual-stage method was developed to first efficaciously degrade metaldehyde into acetaldehyde, before subsequent removal of acetaldehyde using an amine functionalized ion-exchange resin. A range of Macronets, with different surface areas, pore volumes, pore size distributions and extents of functionalisation were evaluated for the depolymerisation of metaldehyde. NMR spectroscopy was used to confirm the compete degradation of metaldehyde by the selected Macronets. Kinetic studies showed that the rates of catalytic degradation were primarily determined by the porous structure of the materials rather than the extent of surface functionalization, since high levels of acid surface groups were observed to decrease the porosity significantly. The rate constants obtained show excellent correlation with non-micro pore volumes, which are of import as the only pores that are accessible to hydrogen bonded metaldehyde molecules; Macronet MN502 exhibits the largest non-micro pore volume and, hence, demonstrated the best kinetic performance. The effect of competing ions on catalytic performance was also studied and the results demonstrate that competing ions compromise the performance of the proposed system to some extent, however, it is notable that a good level of performance is maintained even for competing ion concentrations as high as 100 times that of metaldehyde. Isothermal studies of acetaldehyde onto ion-exchange resin A830, including kinetic evaluation, showed that acetaldehyde could be chemically adsorbed by the resin. Consequently, a dual-column system was proposed, which was determined to effectively degrade metaldehyde (MN502) and remove the resulting by-product, acetaldehyde, via a second fixed bed absorber (A830); this method could easily be adapted to existing facilities in water treatment works, making it very cost-effective and of great practical interest.

Keywords: Metaldehyde; Acetaldehyde; Macronets; Heterogeneous catalyst; Ion-exchange resin

* Corresponding author: Email: ashleigh.fletcher@strath.ac.uk; Tel: +441415482431

1. Introduction

Recent reports of potable water contamination by metaldehyde [1] have drawn public attention to the matter; the maximum concentration of metaldehyde in U.K. drinking water is regulated, according to its role as a pesticide, at 0.1 µg/L (ppb) [2]. In 2010, several British water treatment works detected significant quantities of metaldehyde in their treated waters, reaching up to 1 ppb, i.e. ten times higher than the permitted level [3]. The detection of metaldehyde in drinking water supplies indicates that current methods utilised in the water treatment industry, i.e. Granular Activated Carbon (GAC) beds, are not working effectively and according to research conducted by the Water Research centre (WRc), a virgin GAC bed was exhausted after only 44 days of use, where metaldehyde breakthrough was detected [4]. Our previous research findings indicated that the rapid exhaustion of GAC is caused by the low adsorption capacity of metaldehyde onto GAC and a high leaching tendency [5]. An additional concern in the use of GAC beds is that, although it can lower the concentration of metaldehyde in water initially, GAC can only remove ~30-50% of the total metaldehyde within a water stream, meaning that water contaminated with metaldehyde at levels > 0.15 ppb, even if treated, will still exceed the threshold of 0.1 ppb [4]. The poor performance of GAC for metaldehyde removal is a result of its low adsorption capacity, exacerbated by high leaching tendencies [5]. Recent work has shown an improvement to carbon based systems using the bespoke sorbent Nyex™, however, the process requires a number of cycles to reach high levels of remediation as well as electrochemical regeneration of the sorbent [6].

Investigations using Advanced Oxidation Processes (AOPs) for metaldehyde removal from drinking water have been undertaken by several researchers; AOPs comprise a category of destructive reaction processes, which have demonstrated promising performances for the removal of micro-pollutants. One sub-category of AOP is chemical activation via UV irradiation to generate highly reactive hydroxyl radicals (e.g. H_2O_2, TiO_2 and H_2O_2/ Fe^{3+}) [7-11]. Studies on the degradation of metaldehyde by AOPs using UV/H_2O_2 and UV/TiO_2 revealed that both methods had efficient degradation of metaldehyde with almost identical removal rates (~ 0.007 cm^2 mJ^{-1}) for synthetic laboratory water samples. However, when tested using real water samples, the degradation performance of UV/TiO_2 was completely limited due to the blockage of active sites by background organic substances. In the case of UV/H_2O_2 and real water samples, the rate of degradation was slowed from 0.007 to 0.002 cm^2 mJ^{-1} by background organic matters [12]. Furthermore, more detailed

investigations into the influence of competing organic substances on the performance of UV/H_2O_2 and UV/TiO_2 showed that hydrophobic matter had a greater inhibitory effect than hydrophilic matter [13]. Therefore, UV/H_2O_2 was deemed to be more effective than UV/TiO_2. However, in order to reach the desired metaldehyde removal performance, large quantities of H_2O_2 are required and high UV dosage needed, since irradiation at 254 nm (UV light) does not activate H_2O_2 effectively [12-14]. Although it is was shown that AOP can remove metaldehyde from water, there are still key issues that need to be addressed before it may be employed in large-scale water treatment works, including the issues of by-product production and the prohibitively high infrastructure and running costs of the process [14].

Currently, as discussed above, existing methods for the removal of metaldehyde suffer certain limitations, therefore; alternative cost-effective and more practical methods are urgently required to address metaldehyde contamination within U.K. water supplies. Our previous research has shown that sulfonic acid functionalised silica materials efficiently remove metaldehyde from drinking water[15]; achieved by a mechanism involving the degradation of metaldehyde into acetaldehyde, thereby, creating a secondary pollutant ameliorated using amine functionalised materials in a dual-stage process. Previous fabrication of a bench scale dual-stage system was attempted, however, some obstacles hindered the installation. Obstructions hindering the installation and evaluation of the previously proposed treatment system primary include (1) the large-scale production and commercialisation of the prepared silica samples, which would significant require time to achieve particularly with regards obtaining regulatory permits for potable water; (2) the silica samples, as-synthesised, were in the form of very fine particles (<10 μm), which would cause tremendous pressure drops if used in fixed-bed columns. According to Darcy's law of describing flow in porous media[16], the pressure drop (Δp) of flow through porous material packed column can be calculated by the equation of $\Delta p = (Q \cdot \mu \cdot L)/(k \cdot A)$, where Q is flowrate, μ is viscosity of fluid, L denotes the length of bed, A is area of cross section and k is the permeability (or hydraulic conductivity) of the packed medium. Permeability of the packed material is affected by the particle size and porosity (e.g. pore size) of the material. As indicated by the characterization of silica samples[15], the particle size fell in the range of 1-50 μm and pores were micro and mesoporous, meaning the permeability of the silica packed column would be very small and the pressure drop would be tremendous. Therefore, alternative materials with bigger particle size and large pore sizes could solve these issues, hence, Macronets with sulfonic acid fictionalisation, were, designed and supplied by Purolite® and, utilised in

a dual-stage process. In comparison, the particle size of Macronets was in the range of 500-650 μm which is a common size in water purification applications. Also, the pore volume of Macronet MN502 is more than 0.3 mL/g. Therefore, the pressure drop associated with operation under standard operating parameters is in the normal range, allowing the proposed dual-stage method to be fabricated and tested. The Macronets used were selected on the outcomes of our previous study, which indicated sulfonic acid functionality showed good metaldehyde degrading performance [15], hence, a series of materials with controlled porosity (surface area, total pore volume, pore size distribution) and extent of sulfonic acid functionalisation were synthesised to allow process optimisation, via a highly efficacious dual-stage method for removal of metaldehyde from drinking water.

2. Experimental

Macronet samples were synthesised at Purolite® International, U.K., and are, subsequently, commercially available; six Macronet samples were prepared, in total, with varying porous textures and a range of acid capacities, allowing for optimisation of desirable material characteristics. The materials can be divided into two sub-categories: Macronet (MN) and D code (DC) series. The MN series includes MN500, MN501 and MN502, while the DC series consists of DC564, DC565 and DC566. The key difference between MN and DC materials is the extent of sulfonation to the same parent matrix, which results in a significant variation in the porous textures of the materials. An ion-exchange resin A830, with complex amine functionality, used in the second stage of the method was also supplied by Purolite®. Textural characterization was performed via analysis of nitrogen sorption isotherms (ASAP 2420, Micrometrics) obtained at -196 °C [17], to provide specific surface areas and pore volumes. Pore size distributions were determined by mercury intrusion porosimetry, performed on a PoreMaster® PM-60 instrument (Quantachrome, UK) [18, 19]. Quantification of extents of surface functionalisation was performed using Boehm titration methods [20, 21]. The concentration of metaldehyde and acetaldehyde in water samples were determined by GC and HPLC, respectively; and the detailed analysing conditions are as described in our previous works [15, 22].

Heterogeneous catalytic degradation of metaldehyde, using Macronets with varied sulfonic acid capacities, was performed by adding 200 mg of catalyst to 200 mL of metaldehyde solution with initial concentration 200 mg L^{-1}. Samples were taken at predetermined time intervals, and the concentration

of metaldehyde and acetaldehyde determined. Kinetic parameters were determined for acetaldehyde chemisorption onto A830 by adding 100 mg of adsorbent to 200 mL acetaldehyde solution, with an initial concentration of 20 mg L^{-1}; again samples were taken at pre-selected time intervals. The adsorption isotherm of acetaldehyde onto A830 at 20 °C was determined by bottle-point method [23].

Performances of the dual-stage method were evaluated by rapid small scale column tests (RSSCTs) as depicted in Figure 1. 1 g of MN502, with mean particle size 180 μm, was packed in a glass column (5 cm bed length × 8 mm I.D.) acting as a heterogeneous catalyst. For treatment of the by-product acetaldehyde, 2 g of A830, with particle size 180 μm, was packed into a second column (5 cm bed length × 8 mm I.D.). For the purposes of comparison with traditional treatment methods, two additional fixed-bed systems were fabricated (1) using MN502 as the catalyst but replacing A830 with GAC as the adsorbent for acetaldehyde removal, (2) replacing MN502 with 2 g of GAC to remove metaldehyde with no second column; all remaining system parameters of these additional columns were unchanged. The flow rates for the three sets of apparatus were set at 7 mL/min, resulting in empty bed contact times (EBCTs) of column 1 = 21.5 s and column 2 = 43 s. The initial metaldehyde concentration of the feed solution was 2 mg/L, and the effluents from each column were sampled and analysed.

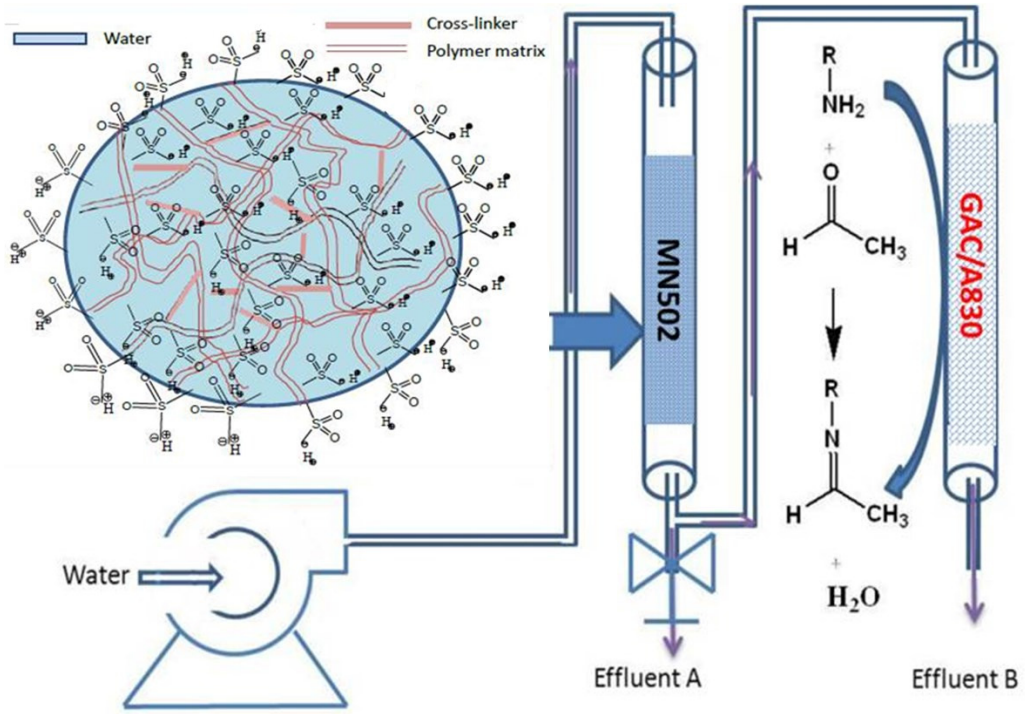

Figure 1: Schematic illustration of the setup of the novel dual-stage column tests used in this study; column 1 packed with either 1 g of Macronet MN502 or 2 g of Granulated Activated Carbon (GAC), column 2 packed with 2 g of either ion exchange resin A830 or GAC.

3. Results and Discussion

3.1 Characterisation of materials

Table 1 summarises the textural properties and acid capacities of the Macronet samples used in this study, and it can be seen that the introduction of sulfonic acid groups reduces the porosity of the samples. The unfunctionalised matrix of these Macronets has a total pore volume of 0.667 cm^3/g and a surface area of 950 m^2/g, according to the manufacturer's specifications, while slightly functionalising the matrix (MN series) decreases both the surface area and pore volume substantially (surface areas 330-400 m^2/g); further functionalisation (DC series) causes additional decrease of the surface area (3-22 m^2/g) and a similar trend in pore volume. In addition to available volume and area, it is also important to consider the trend in pore size, since metaldehyde molecules tend to assemble via hydrogen bonding to form macro-molecular structures; the surface area and pore volume contributed by the meso- and macro-pores is crucial as these are the channels that will facilitate diffusion and removal of the large metaldehyde clusters. Hence, the percentages of meso- and macro-pore volume ($V_{Meso-Macro}$) compared to the total pore volume (V_{Total}) were calculated, and Figure 2 shows the pore size distributions of the MN series samples, as determined by mercury intrusion. It is clearly shown that among the MN samples, MN502 has the largest pore volume, reaching 0.328 $cm^3 g^{-1}$ (**Error! Reference source not found.**). More importantly, the large majority (0.203 $cm^3 g^{-1}$, 62% of total pore volume) of the pore volumes are contributed by non-micropores, meaning most of the pores are accessible to hydrogen bonded metaldehyde molecules (Figure 2). MN501 may well exhibit the highest surface area, reaching 402 $m^2 g^{-1}$ but 300 $m^2 g^{-1}$ of this area is contributed by micropore surfaces; similarly, MN501 has a high total pore volume of 0.310 $cm^3 g^{-1}$ but only half of its 0.158 $cm^3 g^{-1}$ is non-micropore volume. Of the MN series, MN500 has the lowest total pore volume (0.260 $cm^3 g^{-1}$), with the lowest contribution from meso/macropores, as well as a low surface area (331 $m^2 g^{-1}$).

Table 1: Summary of textural properties and acid capacities of the Macronet samples used in this study.

I.D	S_{Total}§	S_{Micro}*	$S_{Meso-Macro}$ (S_{Total}-S_{Micro})	V_{Total}†	V_{Micro}*	$V_{Meso-Macro}$ (V_{Total}-V_{Micro})	Acid capacity‡
	(m^2/g)			(cm^3/g)			(mmol/g)
MN500	332	234	98	0.260	0.120	0.139	2.77
MN501	402	293	109	0.310	0.151	0.158	2.64
MN502	356	242	114	0.328	0.125	0.203	2.74
DC564	22.3	5.2	17.1	0.133	0.003	0.130	2.88
DC565	21.2	4.9	16.3	0.082	0.003	0.080	3.05
DC566	2.6	0.2	2.4	0.007	N/A	0.007	3.34

§ Determined from BET analysis.
† Determined from total uptake at P/P_o ~ 1.
* Determined from t-plot.
‡ Determined from Boehm titration method.

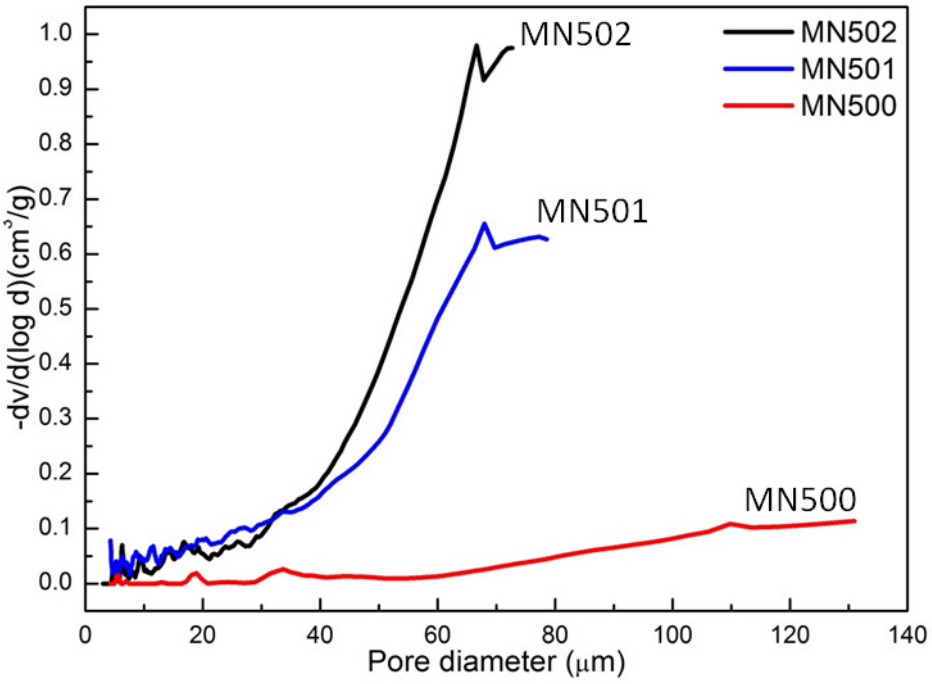

Figure 2: Pore size distributions of the MN series Macronets used in this study: MN500 (—), MN501 (—), MN502 (—), as determined by the BJH method applied to N_2 desorption isotherms obtained at -196°C.

3.2 Catalysis selectivity study

Previous results have demonstrated that sulfonic acid functionalities have the ability to degrade metaldehyde into acetaldehyde, efficiently and completely [15]. In order to determine the level of efficiency of the catalytic materials used in this study, Nuclear Magnetic Resonance (NMR) tests were conducted to probe the presence of metaldehyde after degradation using the series of Macronets. 20

mg of metaldehyde was dissolved in 50 mL of deuterated water (D_2O). The NMR spectrum for the initial metaldehyde/deuterated water mixture was recorded and is displayed in Figure 3 as 'Before'. 2 mg of the best performing Macronet MN502 was then added into the solution, and the NMR spectrum was taken again after 15 min of shaking / reaction and is displayed in Figure 3 as 'After'. More spectra were recorded at different time intervals but do not show any additional products. It is clear that peaks corresponding to metaldehyde (d at 1.4 ppm, q at 5.4 ppm) decreased to almost negligible levels as reaction time elapsed and only characteristic peaks of acetaldehyde (d at 2.2 ppm, s at 9.6 ppm) were observed, confirming substantial degradation of metaldehyde into acetaldehyde with no further intermediates or by-products.

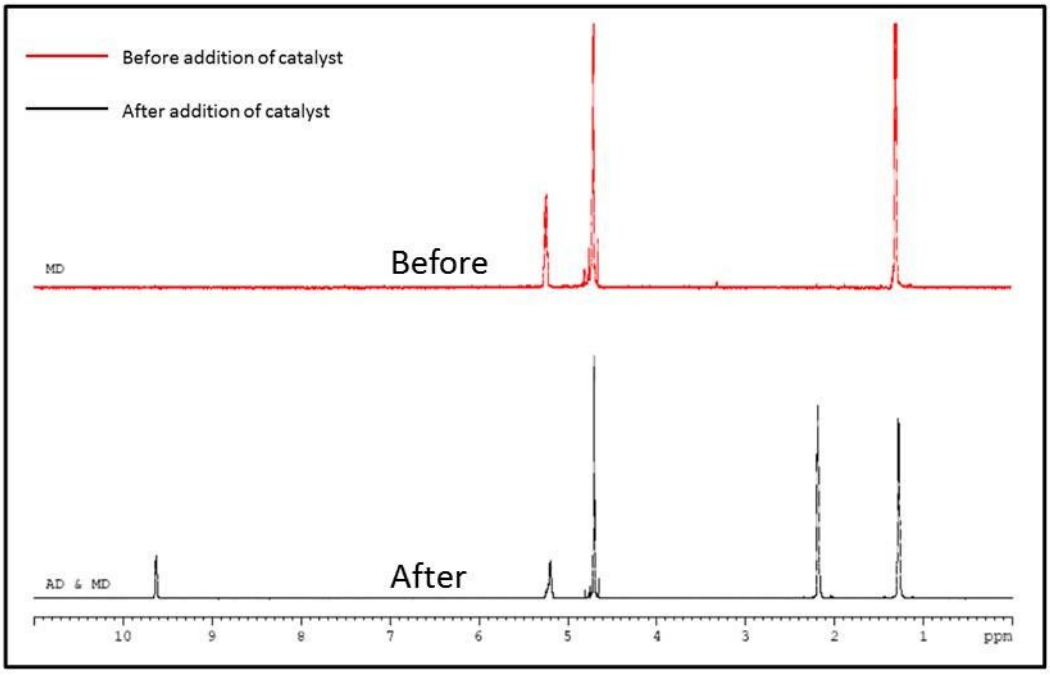

Figure 3: NMR spectra of a metaldehyde (in D_2O) solution before (─) and after (─) addition of Macronet MN502, showing the presence of metaldehyde (MD; d:1.4 ppm, q:5.4 ppm) and acetaldehyde (AD; d:2.2 ppm, s:9.6 ppm).

Considering these results in conjunction with our previous results**,** it is clear that the mechanism for degradation of metaldehyde by Macronets is the same as that proposed for sulfonated silica (SBA-15), with the sulfonic acid functionalised Macronet acting as a heterogeneous catalyst, effectively depolymerising metaldehyde into acetaldehyde.

3.3 Catalysis kinetic study

As the process is catalytic, it is vitally important to investigate the reaction kinetic performance

of the heterogeneous catalysts used in this study; hence, comparative kinetic experiments were conducted. The depolymerisation reaction can be described by the following kinetic equations:

$$\mathbf{C_8H_{16}O_4\ (MD) \xrightarrow{RSO_3H} 4\ CH_3CHO(AD)} \qquad \text{Eq. (1)}$$

$$\mathbf{r = -\frac{d[MD]}{dt} = k[MD][RSO_3H]} \qquad \text{Eq. (2)}$$

Since the concentration of sulfonic acid is constant and in significant excess, the overall rate of reaction is only dependent on the concentration of metaldehyde, thus, Eq. (2) becomes a first order rate equation [24] with the integrated formula being expressed as:

$$\frac{c_t}{c_0} = e^{-kt} \qquad \text{Eq. (3)}$$

The trend in metaldehyde concentration as a function of time is shown in Figure 4, with different Macronets acting as catalysts under the same experimental conditions; also shown are the curves obtained for the raw experimental data being fitted to a theoretical first order rate equation. The kinetic parameters obtained are summarized in Table 2.

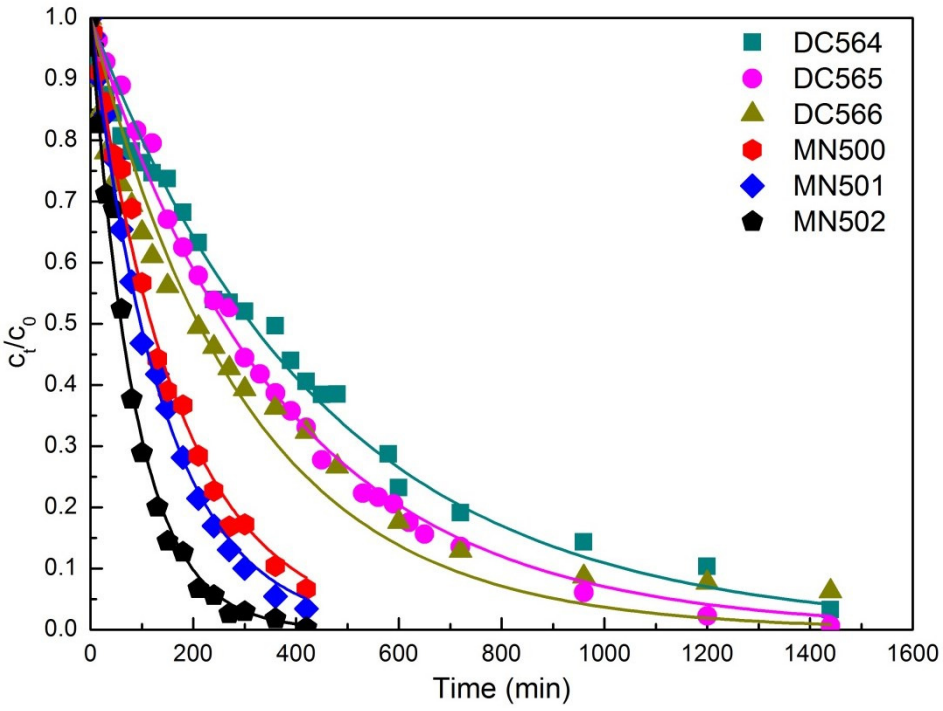

Figure 4: Kinetics of metaldehyde degradation by different Macronet catalysts used in this study: DC564 (■), DC565 (●), DC566 (▲), MN500 (μ), MN501 (♦), MN502 (□), measurements conducted at 22 °C. Fits shown are for first order rate equations (solid lines).

The capacity of the Macronet materials appears to be limited only by the initial concentration used for the remediation study, here 200 ppm, which translates to 200 mg/g and this is significantly higher than previously reported capacities for adsorption on a phenolic carbon (76 mg/g) [25], and is

supported by the higher capacity previously observed for catalytic degradation by an ion exchange resin [5]. Generally, it can be seen that MN samples exhibit much faster kinetics than DC samples, with rate constants (k) 3-4 times higher; this can be ascribed to the fact that MN samples have textual properties much better suited to the target system, i.e. larger surface areas and highly meso/macroporous volumes, compared to DC samples. These properties increase the permeability of the MN Macronets, facilitating the path of metaldehyde molecules to diffuse to the active sites with the materials. The results also indicate that an increasingly high extent of functionalisation is not necessary because the further functionalized DC samples demonstrated significantly poorer kinetics. Within a heterogeneous catalysis process, the diffusion step is always the rate-limiting step, whereas the reaction step is, by comparison, very fast. The high acid capacities of the DC samples markedly decreases sample porosity, resulting in an increase in diffusive resistance towards metaldehyde clusters. Therefore, the rates of catalysis are very slow, as the metaldehyde has hindered diffusion to the active sites, despite the fact that their densities are correspondingly high.

Table 2: Parameters obtained by fitting experimental kinetic data obtained for the degradation of metaldehyde using a series of Macronet materials to first order kinetic equations.

Macronets	MN500	MN501	MN502			DC564	DC565	DC566
T (°C)	22	22	22	25	30	22	22	22
k ($\times 10^{-3}$ min^{-1})	5.86	7.11	11.6	16.3	24.8	2.22	2.65	3.31
R^2	0.99	0.98	0.99	0.99	0.99	0.98	0.99	0.93

Comparison of the kinetic data obtained at 22 °C for three MN samples, shows that the best kinetic performance was achieved using MN502, which possesses the largest pore volume. MN501 has the highest surface area but gave a much lower rate constant. Close examination of the kinetics determined for the MN samples, shows that, as predicted, pore volume, especially meso and macro pore volume, is more desirable than surface area. Figure 5 presents the correlations between rate constant and textural characteristics, including surface area, total pore volume and non-micro pore volume among the MN samples; a positive linear relationship is only observed for the correlation of rate constant to meso and macro pore volume, indicating that non-micropores play a significant role in the catalytic process due to the increased size of the hydrogen-bonded macromolecular structure of metaldehyde [26], as micropores will not be accessible to these extended molecular structures. It is, therefore, implicit that the principal reason that Granular Activated Carbons (GACs) show poor

performances for metaldehyde removal, is as a consequence of the majority of the porosity present in GAC materials being microporous.

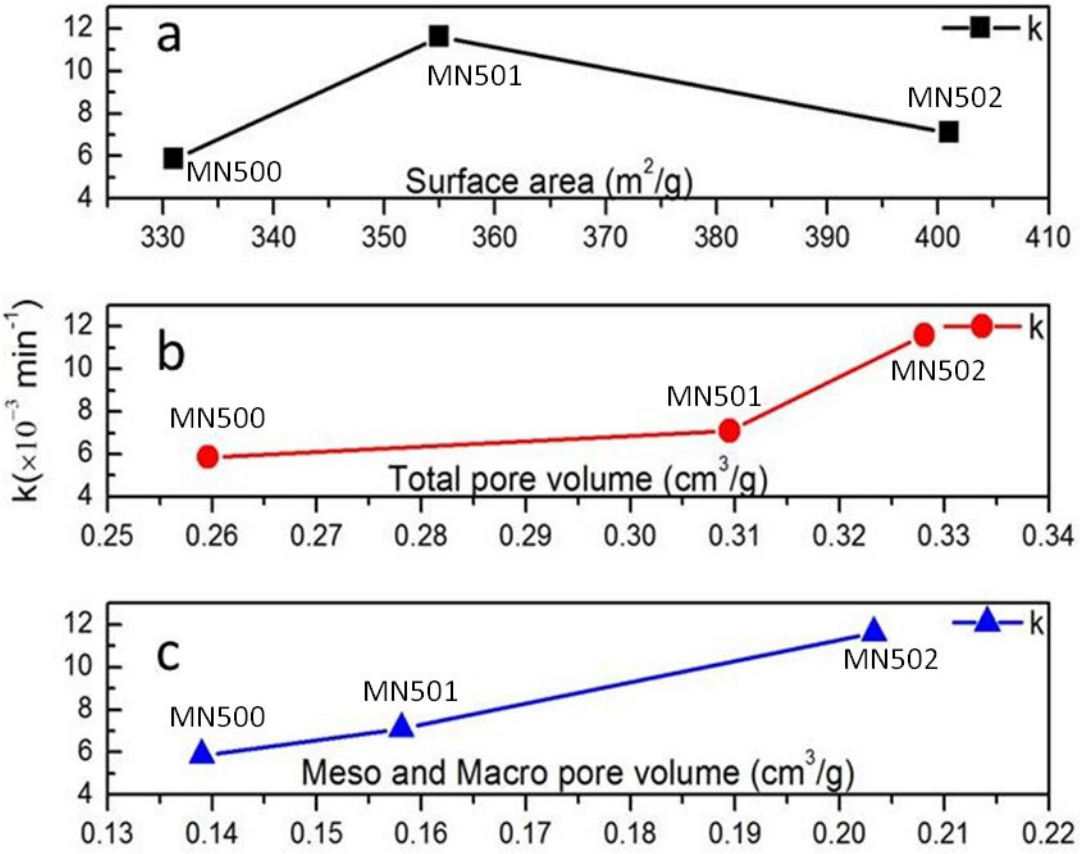

Figure 5: Correlations of rate constant of metaldehyde degradation at 22°C to (a) surface area (—■—), (b) total pore volume (—●—) and (c) combined meso- and macropore volume (—▲—) for MN Macronet samples used in this study, .

The Arrhenius equation [27] states that the rate constants of a process demonstrate a temperature dependence, from which the activation energy of a catalytic process (E_a, kJ mol^{-1}) can be estimated:

$$ln\mathrm{k} = lnA - \frac{E_a}{RT} \qquad \text{Eq. (4)}$$

Figure 6 presents the catalytic reaction kinetics for metaldehyde degradation by MN502 at three different temperatures, with the calculated rate constants for each temperature shown in Table 2. The resulting activation energy, from the linearised plot of ln*k* versus 1/T, is 75.4 kJ mol^{-1}, confirming that the process is both an endothermic and chemical one.

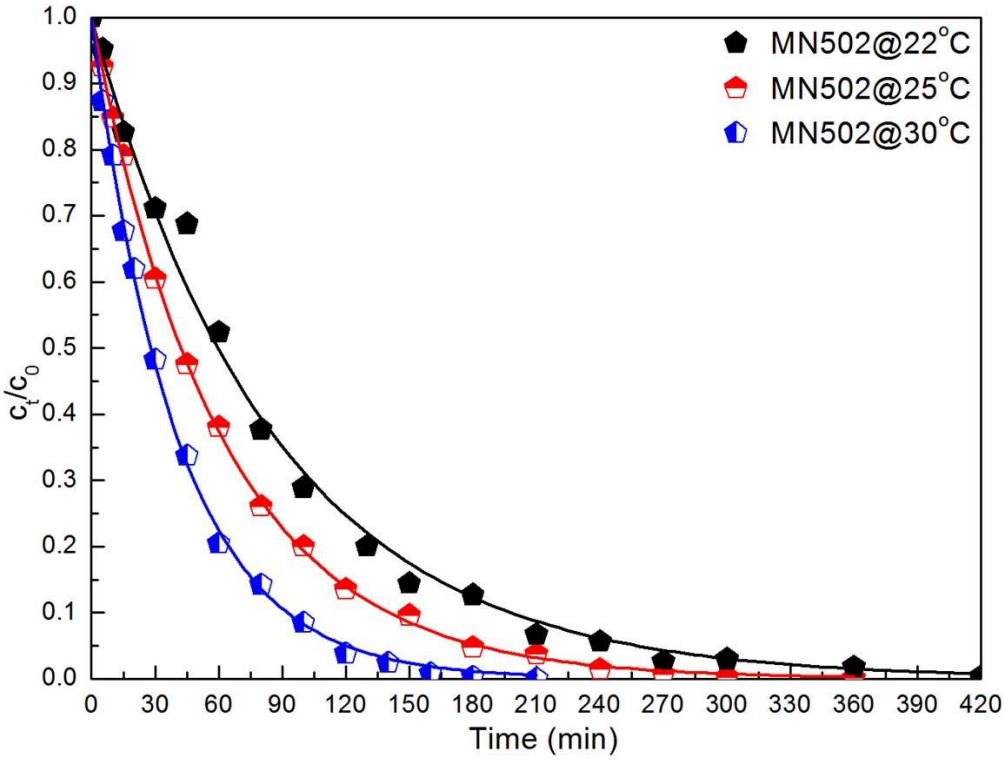

Figure 6: Temperature dependence of catalytic performance of metaldehyde degradation by Macronet MN502 at 22 °C (□), 25 °C (□) and 30 °C (□), also showing fits of experimental data to theoretical first order rate equations (solid lines).

3.4 Competing effect of inorganic ions on catalytic performance

It is generally recognised that the presence of inorganic ions causes significant effects on adsorption and catalytic processes in water treatment [28, 29]. In this study, the effect of calcium ions (Ca^{2+}) on the degradation of metaldehyde was investigated, since Ca^{2+} is the major inorganic ion in drinking water, especially in U.K. regions that experience high levels of metaldehyde contamination. Figure 7 shows the effect of different concentrations of Ca^{2+} on the kinetics and capacities of the metaldehyde depolymerisation reaction, using MN502. It is clear that the presence of calcium ions decreases both the reaction rate and the overall capacity significantly, with an increased impact observed at high Ca^{2+} concentration; however, the effect plateaus with increasing concentration ratio of Ca^{2+}/metaldehyde, even for ratios as high as 100 times.

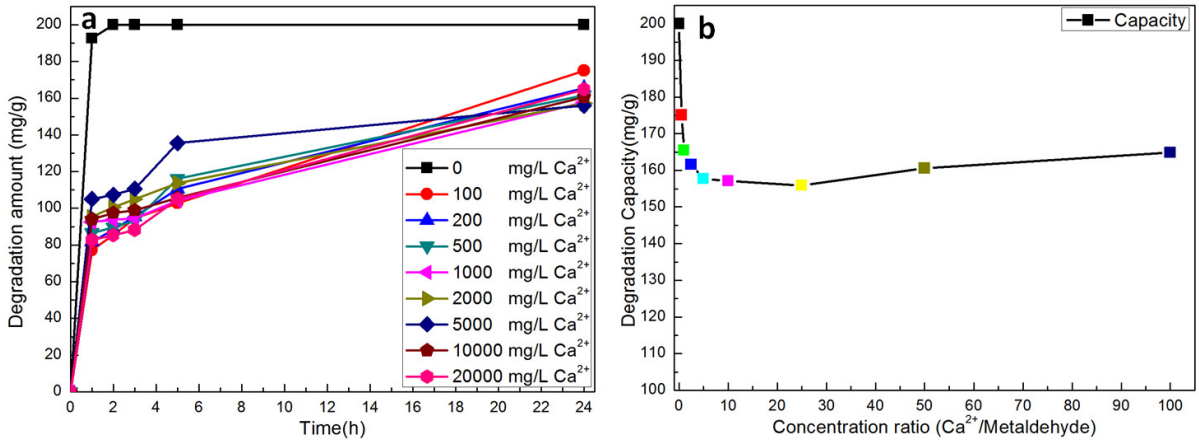

Figure 7: Effect of competing ions (Ca^{2+}: 0-20000 mg/L) on metaldehyde degradation (initial concentration 200 ppm) using Macronet MN502: (a) kinetic performance over 24 h; (b) total capacities at 24 h.

The experimental results obtained demonstrate that the presence of inorganic ions decreases both the kinetics and capacities of Macronet MN502, which can be explained by consideration of the different working mechanisms of the sulfonic acid group interactions with metaldehyde and inorganic ions. For inorganic ion remediation processes, the working mechanism is ion-exchange, while for metaldehyde removal; the process is a catalytic reaction, as illustrated in Figure 8. As is generally recognised, every ion-exchange reaction is reversible with the equilibrium constant highly dependent on the ion pairs. In industrial water treatment processes, sodium forms of resins are normally used to soften water [30-32], rather than the proton forms, as the bonding energy between RSO_3^- and H^+ is much stronger than that between RSO_3^- and Na^+, such that breaking RSO_3-H is more difficult than breaking RSO_3-Na. Hence, for the ion-exchange process between MN502 and Ca^{2+}, the rate constant is expected to be low, so that, even at equilibrium, there is some RSO_3H remaining. As long as some RSO_3H is available, it will continue to catalyse the degradation of metaldehyde; hence, despite the high ratios of Ca^{2+}/metaldehyde, the catalytic degradation mechanism is still available. Using these results as a basis, it is possible to predict that for an implemented fixed-bed column packed with Macronet, inorganic ions will initially be absorbed by the column via ion-exchange, as well as the simultaneous degradation of metaldehyde; the bed will then reach its capacity for the inorganic ion and be unable to adsorb further Ca^{2+} ions, however, the remaining RSO_3H will still be available to degrade metaldehyde, albeit with slower reaction kinetics.

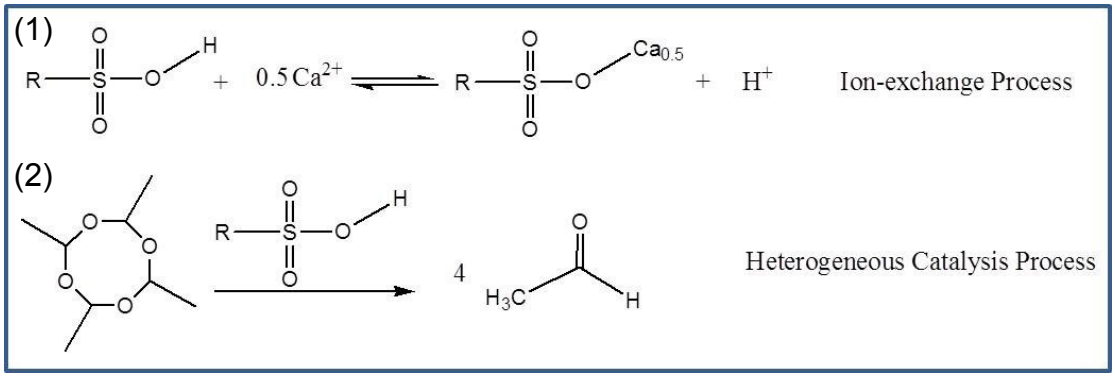

Figure 8: Proposed mechanism for roles of sulfonic acid groups in (1) removal of inorganic ions by ion-exchange and (2) metaldehyde degradation by heterogeneous catalysis.

3.5 Removal of acetaldehyde by ion-exchange resin A830

It has been reported in the literature that aldehydes can be removed using primary amines, as a result of a condensation reaction [33, 34]:

$$\boldsymbol{R - NH_2 + CH_3CHO \xrightarrow{yields} CH_3CH = N - R + H_2O} \qquad \text{Eq. (5)}$$

Therefore, in this work, an amine functionalised resin with acrylic matrix has been applied to remove the acetaldehyde produced in the first reaction step of the process presented here. Figure 9a shows kinetic data obtained for acetaldehyde adsorption onto A830; data obtained for acetaldehyde adsorption onto GAC is included for comparison. It is clear that the kinetics of acetaldehyde adsorption onto A830 are much faster than those for GAC. More than 90% of available acetaldehyde was absorbed by A830 within 8 h. The kinetic data were better described by a pseudo-second order equation, with a rate constant of 0.170 g mg^{-1} min^{-1}. With regards to the adsorption of acetaldehyde onto GAC, the performance was quite poor, which is ascribed to the weak physical interactions between GAC and acetaldehyde.

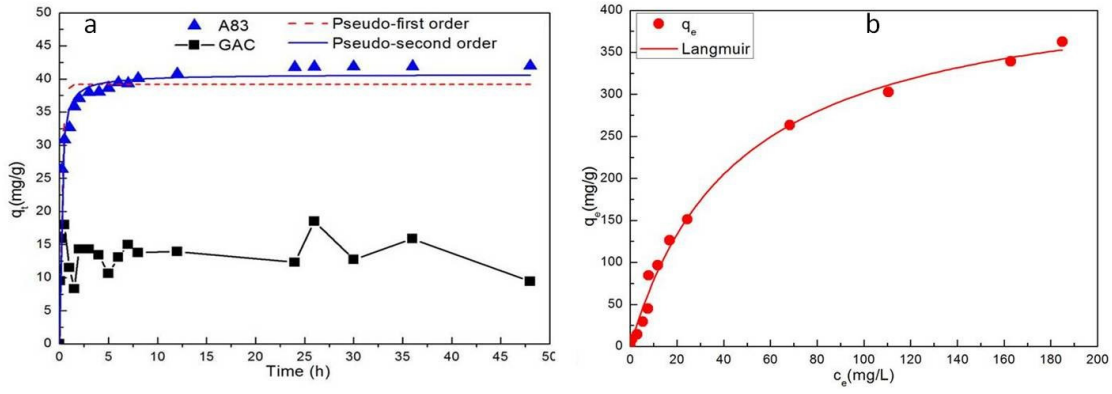

Figure 9: (a) Adsorption kinetics of acetaldehyde onto ion exchange resin A830 (—▲—) [35] and Granular Activated Carbon, GAC (—■—) at 20 °C, including fits of the data to pseudo-first (---) and pseudo-second (—) kinetic models; (b) Isotherm of acetaldehyde sorption onto A830 at 20 °C (—●—) [15], also showing the fit of the data to the Langmuir equation (—).

Since the kinetic adsorption performance of A830 was much better than that of GAC, the isotherm of acetaldehyde sorption onto A830 was investigated. Figure 9b shows the isotherm obtained at 20 °C and the theoretical curve generated by the Langmuir equation; this model assumes monolayer adsorption and is suited to this work as the proposed mechanism requires acetaldehyde molecules to diffuse to the adsorbent surface and react with surface functional groups via the condensation reaction shown above [36-38]. Consequently, the Langmuir equation is widely used to describe sorption of solutes onto heterogeneous surfaces involving surface functionalities and adsorbate-adsorbent interactions:

$$q_e = q_m K_L C_e / (1 + K_L C_e) \qquad \text{Eq. (6)}$$

The fit obtained shows that the experimental data were in good agreement with the theoretical model, hence, also in agreement with the proposed adsorption mechanism, giving a high maximum adsorption capacity (q_m, mg g^{-1}) of 441 mg g^{-1}, indicating that A830 is good candidate for acetaldehyde removal.

3.6 Dual-stage column tests

The batch experiments discussed above demonstrate that metaldehyde can be efficiently degraded into acetaldehyde by sulfonic acid functionalised Macronets, and the acetaldehyde produced can be removed by amine functionalised ion-exchange resins. Therefore, a dual-stage fixed-bed absorber (FBA) was fabricated with the first column packed with catalyst MN502 and the second packed with adsorbent A830. For comparison to traditional water treatment systems, three

column tests were conducted: (1) single-column setup with column packed with GAC; (2) dual-column setup with first column packed with MN502 and second with A830; (3) dual-column setup with first column packed with MN502 and second with GAC. The operating conditions and parameters were kept the same as detailed in the experimental section.

Figure 10 demonstrates the breakthrough curves obtained for the three column tests. The profiles shown in Figure 10 represent the final effluent concentration, i.e. in single-column setup it is the metaldehyde concentration, while the acetaldehyde concentration is shown for both dual-column setups. For the single-column setup, it can be seen that the bed was exhausted quickly and the concentration of the effluent reached more than 90% of its initial influent concentration after only 24 h of operation. This agrees with the results obtained from application of GAC in the water treatment industry, caused by the low adsorption capacity and high leaching tendency of metaldehyde adsorption onto GAC. The dual-column configurations, showed that no metaldehyde was detected over the whole running time, indicating good degradation performance of MN502. In the case of using GAC to remove acetaldehyde, the breakthrough of the GAC bed was quickly observed, suggesting this material is not appropriate to adsorb acetaldehyde, and lending weight to the development of alternative methods for its removal should future legislation require a reduction in acetaldehyde concentration. The dual-column setup consisting of MN502 and A830 showed excellent amelioration performance. It took 60 h (5,000 bed volumes (BV)) to reach the 10% of c_t/c_0 threshold. In this experiment, the initial concentration of metaldehyde was 2 ppm which is 2,000 times higher than the maximum concentration (1 ppb) detected in water catchments. Therefore, in practical cases, the breakthrough point of the dual-column should be expected to be much better than 5,000 BV, hence, this dual-column configuration shows very promising results. The bed completely removed acetaldehyde for the first 3,000 BV of water before breakthrough was detected. The bed was not exhausted after 10 d running and the concentration ratio only reached 40%. The column tests are in good agreement with the batch experiment results, with the dual-columns showing robust performance, as expected. The method developed here is of practical interest for the removal of metaldehyde from drinking water supplies.

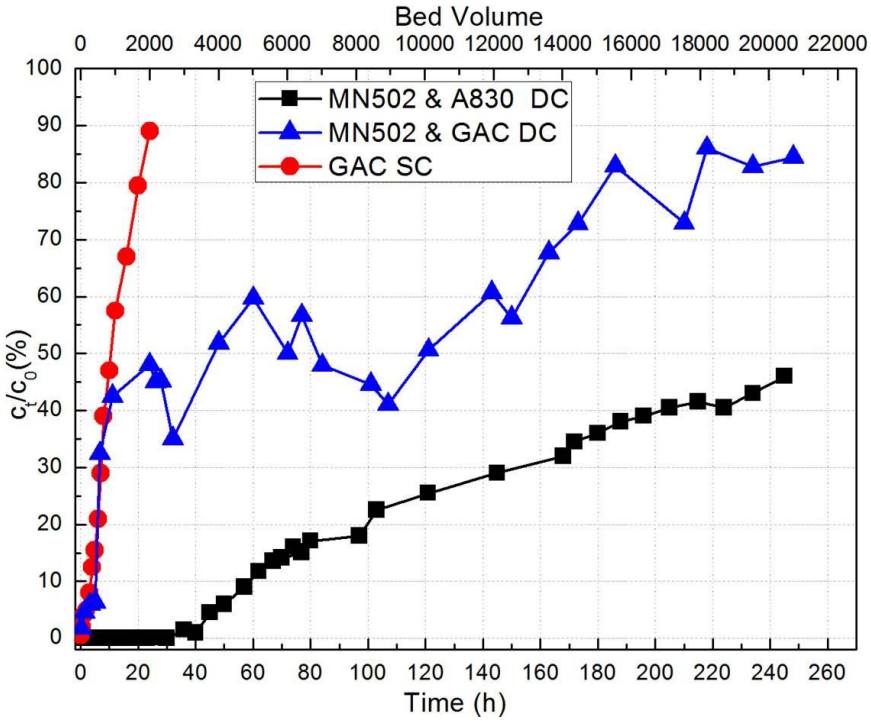

Figure 10: Breakthrough curves of the three fixed-bed absorbers used for metaldehyde degradation. Setup 1: Single Column (SC) Granular Activated Carbon (—●—); Setup 2: Dual Column (DC) Macronet MN502 and ion exchange resin A830 (—■—). Setup 3: DC MN502 and GAC (—▲—).

4 Conclusions

Efficacious metaldehyde removal was achieved by the application of a combination of macroporous sulfonic functionalised Macronet, as catalyst, and amine functionalised ion-exchange resin, as adsorbent. NMR analysis confirmed that heterogeneous catalysis of metaldehyde was substantial with acetaldehyde the only by-product. Kinetic studies revealed that the rate of metaldehyde degradation is determined by the diffusional step and a high extent of functionalisation is not necessarily required to obtain good catalytic performance, since the introduction of functional groups significantly compromises the porosity. The kinetic study also revealed that the degradation rate is closely related to the total pore volume, especially to the meso- and macropore volumes. Macronet sample MN502, with considerable surface area, appropriate pore size and large pore volume showed the best kinetic performance; the fast kinetics observed for MN502 are related to the effective accessibility of metaldehyde molecules to the sulfonic acid groups present in the sample. Competing ion tests showed that the presence of inorganic ions (Ca^{2+}) decreased the catalytic

performance, however, good level of degradation (~80%) was observed even with Ca^{2+} concentrations 100 times those of metaldehyde; this limited influence is the result of the interaction between sulfonic acid groups and Ca^{2+} being an ion-exchange process, sulfonic acid groups and metaldehyde undergo heterogeneous catalytic processes. The kinetic and isothermal studies of acetaldehyde onto resin A830 demonstrated that the only by-product of metaldehyde degradation can be effectively removed. Breakthrough curves for the fabricated dual-column system confirmed the effective degradation of metaldehyde by MN502 and the complete removal of acetaldehyde by a second bed packed with ion-exchange resin A830. The method developed in this work is very promising since it can be used in conjunction with existing infrastructure in U.K. water treatment works making the process cost-effective and easy to apply.

Acknowledgements

The authors are thankful to Purolite (Llantrisant, UK) for supply of Macronets and resin A830. B.T. thanks the China Scholarship Council (CSC) and the University of Strathclyde for financial support.

References

[1] R. Edwards, Slug-killing pellets blamed for Scottish water contamination, in: Herald Scotland, Herald & Times Group, Scotland, 2010.
[2] Water England and Wales, The Water Supply (Water Quality) Regulations 2000, Water England and Wales., United Kingdom, 2000.
[3] Jim Marshall, Water UK Briefing Paper on Metaldehdye in, Water UK, London, 2013.
[4] T. Hall, Holden, B., Haley, J.,, Removal of metaldehyde and other pesticides., in: 4th Developments in Water Treatment and Supply Conference, WRc, Cheltenham, 2011.
[5] B. Tao, A.J. Fletcher, Metaldehyde removal from aqueous solution by adsorption and ion exchange mechanisms onto activated carbon and polymeric sorbents, J.Hazard. Mater., 244 (2013) 240-250.
[6] M.A. Nabeerasool, A.K. Campen, D.A. Polya, N.W. Brown, B.E. van Dongen, Removal of Metaldehyde from Water Using a Novel Coupled Adsorption and Electrochemical Destruction Technique, Water, 7 (2015) 3057-3071.
[7] S. Parsons, Advanced oxidation processes for water and wastewater treatment, IWA publishing, London, 2004.
[8] S. Sanches, M.T.B. Crespo, V.J. Pereira, Drinking water treatment of priority pesticides using low pressure UV photolysis and advanced oxidation processes, Water Res., 44 (2010) 1809-1818.
[9] C.M. Sharpless, K.G. Linden, Experimental and model comparisons of low-and medium-pressure Hg lamps for the direct and H_2O_2 assisted UV photodegradation of N-nitrosodimethylamine in simulated

drinking water, Environ. Sci. Technol., 37 (2003) 1933-1940.
[10] J. Thomson, F. Roddick, M. Drikas, Natural organic matter removal by enhanced photo-oxidation using low pressure mercury vapour lamps, Water Supp., 2 (2002) 435-443.
[11] B. Toepfer, A. Gora, G.L. Puma, Photocatalytic oxidation of multicomponent solutions of herbicides: Reaction kinetics analysis with explicit photon absorption effects, App. Catal. B - Environ., 68 (2006) 171-180.
[12] O. Autin, J. Hart, P. Jarvis, J. MacAdam, S.A. Parsons, B. Jefferson, Comparison of UV/TiO_2 and UV/H_2O_2 processes in an annular photoreactor for removal of micropollutants: influence of water parameters on metaldehyde removal, quantum yields and energy consumption, Appl. Catal. B - Environ., 138 (2013) 268-275.
[13] O. Autin, J. Hart, P. Jarvis, J. MacAdam, S.A. Parsons, B. Jefferson, The impact of background organic matter and alkalinity on the degradation of the pesticide metaldehyde by two advanced oxidation processes: UV/H_2O_2 and UV/TiO_2, Water Res., 47 (2013) 2041-2049.
[14] O. Autin, J. Hart, P. Jarvis, J. MacAdam, S.A. Parsons, B. Jefferson, Comparison of UV/H_2O_2 and UV/TiO_2 for the degradation of metaldehyde: kinetics and the impact of background organics, Water Res., 46 (2012) 5655-5662.
[15] B. Tao, A.J. Fletcher, Catalytic degradation and adsorption of metaldehyde from drinking water by functionalized mesoporous silicas and ion-exchange resin, Sep. Purif. Technol., 124 (2014) 195-200.
[16] S. Whitaker, Flow in porous media I: A theoretical derivation of Darcy's law, Transport Porous Med., 1 (1986) 3-25.
[17] E.P. Barrett, L.G. Joyner, P.P. Halenda, The determination of pore volume and area distributions in porous substances. I. Computations from nitrogen isotherms, J. Am. Chem. Soc., 73 (1951) 373-380.
[18] H. Giesche, Mercury porosimetry: a general (practical) overview, Par. Part. Syst. Char., 23 (2006) 9-19.
[19] S.S. Manickam, J.R. McCutcheon, Characterization of polymeric nonwovens using porosimetry, porometry and X-ray computed tomography, J. Membrane Sci., 407 (2012) 108-115.
[20] S.L. Goertzen, K.D. Thériault, A.M. Oickle, A.C. Tarasuk, H.A. Andreas, Standardization of the Boehm titration. Part I. CO_2 expulsion and endpoint determination, Carbon, 48 (2010) 1252-1261.
[21] A.M. Oickle, S.L. Goertzen, K.R. Hopper, Y.O. Abdalla, H.A. Andreas, Standardization of the Boehm titration: Part II. Method of agitation, effect of filtering and dilute titrant, Carbon, 48 (2010) 3313-3322.
[22] B. Tao, A.J. Fletcher, Metaldehyde removal from aqueous solution by adsorption and ion exchange mechanisms onto activated carbon and polymeric sorbents, Journal of Hazardous Materials, 244 (2013) 240-250.
[23] J.C. Crittenden, S. Sanongraj, J.L. Bulloch, D.W. Hand, T.N. Rogers, T.F. Speth, M. Ulmer, Correlation of aqueous-phase adsorption isotherms, Environ. Sci. Technol., 33 (1999) 2926-2933.
[24] L.-n. Shi, X. Zhang, Z.-l. Chen, Removal of chromium (VI) from wastewater using bentonite-supported nanoscale zero-valent iron, Water Res., 45 (2011) 886-892.
[25] R. Busquets, O.P. Kozynchenko, R.L. Whitby, S.R. Tennison, A.B. Cundy, Phenolic carbon tailored for the removal of polar organic contaminants from water: A solution to the metaldehyde problem?, Water Res., 61 (2014) 46-56.

[26] S.A. Barnett, A.T. Hulme, D.A. Tocher, A low-temperature redetermination of metaldehyde, Acta Crystallogr. E, 61 (2005) 857-859.
[27] J.H. Flynn, L.A. Wall, A quick, direct method for the determination of activation energy from thermogravimetric data, J. Polym. Sci. Pol. Lett., 4 (1966) 323-328.
[28] K. Vermöhlen, H. Lewandowski, H.-D. Narres, M. Schwuger, Adsorption of polyelectrolytes onto oxides—the influence of ionic strength, molar mass, and Ca^{2+} ions, Colloid Surface A, 163 (2000) 45-53.
[29] M.E. Parolo, M.J. Avena, G.R. Pettinari, M.T. Baschini, Influence of Ca^{2+} on tetracycline adsorption on montmorillonite, J. Colloid Interf. Sci., 368 (2012) 420-426.
[30] J.N. Apell, T.H. Boyer, Combined ion exchange treatment for removal of dissolved organic matter and hardness, Water Res., 44 (2010) 2419-2430.
[31] A. Swelam, A. Salem, M. Awad, Permanent Hard Water Softening Using Cation Exchange Resin in Single and Binary Ion Systems, World J. Chem., 8 (2013) 01-10.
[32] W. Rieman, H.F. Walton, Ion Exchange in Analytical Chemistry: International Series of Monographs in Analytical Chemistry, Elsevier, 2013.
[33] A.M. Ewlad-Ahmed, M.A. Morris, S.V. Patwardhan, L.T. Gibson, Removal of Formaldehyde from Air Using Functionalized Silica Supports, Environ. Sci. Technol., 46 (2012) 13354-13360.
[34] T. Hayashi, M. Kumita, Y. Otani, Removal of acetaldehyde vapor with impregnated activated Carbons: Effects of steric structure on impregnant and acidity, Environ. Sci. Technol., 39 (2005) 5436-5441.
[35] B. Tao, A.J. Fletcher, Catalytic Degradation and Adsorption of Metaldehyde from Drinking Water by Functionalized Mesoporous Silicas and Ion-Exchange Resin, Separation and Purification Technology, In Press (2014).
[36] I. Langmuir, Chemical reactions at low pressures, J. Am. Chem. Soc., 37 (1915) 1139-1167.
[37] D. Ding, Y. Zhao, S. Yang, W. Shi, Z. Zhang, Z. Lei, Y. Yang, Adsorption of cesium from aqueous solution using agricultural residue–Walnut shell: Equilibrium, kinetic and thermodynamic modeling studies, Water Res., 47 (2013) 2563-2571.
[38] C.W. Davis, D.M. Di Toro, Modeling Non-linear Adsorption to Carbon with a Single Chemical Parameter: A Lognormal Langmuir Isotherm, Environ. Sci. Technol., (2015 DOI: 10.1021/es5061963).